Desalination and Water Treatment
www.deswater.com

doi: 10.1080/19443994.2015.1039597

57 (2016) 10710–10722
May

Taylor & Francis
Taylor & Francis Group

Adsorptive removal of Ni(II) from aqueous solution on 110-H resin: optimization through response surface methodology

Yanli Li[a], Suguo Zhou[a], Lei Fang[b], Jionghui Li[c], Xuming Zheng[d], Jianxiong Jiang[e], Chunhua Xiong[a,*]

[a]*Department of Applied Chemistry, Zhejiang Gongshang University, No. 149 Jiao gong Road, Hangzhou 310012, P.R. China, Tel. +86 15700070475; email: Liyanli361@163.com (Y. Li), Tel. +86 15868163544; email: guiji478@163.com (S. Zhou), Tel. +86 571 88071024, ext. 7571; email: xiongch@163.com (C. Xiong)*

[b]*Department of Food Science and Human Nutrition, University of Florida, Bldg 475 Newell Drive, Gainesville, FL 32611, USA, Tel. +1 352 281 4990; email: fl281218@ufl.edu*

[c]*School of Environmental Science and Engineering, Zhejiang Gongshang University, Hangzhou 310012, P.R. China, Tel. +86 15700070469; email: 1206301806@qq.com*

[d]*Engineering Research Center for Eco-Dyeing & Finishing of Textiles, Ministry of Education, Zhejiang Sci-Tech University, Hangzhou 310018, P.R. China, Tel. +86 0571 86843699; email: zxm@zstu.edu.cn*

[e]*Key Laboratory of Organosilicon Chemistry and Material Technology of Ministry of Education, Hangzhou Normal University, Hangzhou 310018, P.R. China, Tel. +86 0571 28868195; email: fgeorge@21cn.com*

Received 3 July 2014; Accepted 3 April 2015

ABSTRACT

The Box–Behnken design of the response surface methodology was employed to optimize three most important adsorption parameters (initial Ni(II) concentration, pH, and adsorption temperature) and to investigate the interactive effects of these variables on Ni(II) adsorption capacity of 110-H resin. According to analysis of variance and response surface analyses, the experiment data were excellently fitted to the quadratic model. The corresponding optimal parameters of adsorption process are listed as following: temperature at 35°C, initial pH of 6.57, and initial Ni(II) concentration of 0.33 mg/mL. Under optimum adsorption conditions, the adsorption capacity of Ni(II) was 188.5 mg/g, in well accordance with the predicted value by the model (192.88 mg/g). The adsorption kinetics and equilibrium data were well fitted to the pseudo-second-order model and the Langmuir isotherm model, respectively. Thermodynamic parameters (ΔG, ΔS, and ΔH) suggested that the adsorption process was endothermic and spontaneous in nature. Desorption study revealed that Ni(II) can be effectively eluted by 2.0 mol/L HCl solution, and the recovery was 100%. The characterization by Fourier Transform infrared and SEM was performed. Meanwhile, the 110-H resin has been successfully applied in the removal of Ni(II) in natural water samples with satisfactory results.

Keywords: 110-H resin; Ni(II); Adsorption mechanism; Thermodynamic; Response surface methodology

*Corresponding author.

1. Introduction

Heavy metal pollution from industrial wastewater is currently a serious environmental problem [1]. Heavy metals, such as Mn, Cr, Ni, Cu, Hg, and Cd, are common pollutants in industrial wastewater. Due to unique physical and chemical properties, nickel and its compounds are widely used in modern industry, including mineral processing, production of paints and batteries, and manufacturing of sulfate [2]. Nickel and its water-soluble ions are classified as hazardous waste and are highly toxic to plants microorganisms and animals including human beings [3]. Nickel tends to accumulate in the tissues of organisms, causing various diseases, including severe damage to lungs, kidneys, gastrointestinal distress, vomiting, pulmonary fibrosis and skin dermatitis [4]. Nickel has also been identified as a carcinogen [5]. Therefore, the removal of Ni(II) ions from industrial wastewater is particularly important to protect the environment and public health.

In order to remove heavy metal ions from aqueous solutions, several methods have been used, including solvent extraction, chemical oxidation or reduction, co-precipitation, ion-exchange, membrane separation, filtration, electrochemical treatment, and adsorption [6–10]. Some common problems associated with these technologies have limited their industrial applications. For instance, the precipitation methods generate a large amount of sludge causing significant increase in treatment cost. The membrane system always has high treatment cost owing to the frequent change of membranes. Compared with other methods, adsorption via ion-exchange mode has received increasingly more attention in water purification applications due to its unique advantage including good stability, low cost, high capacity for certain metal ions, and the capacity of being reused for many times [11]. Selection of an adsorbent is the key point for developing a proper adsorption technology as the specific type of adsorbent plays a dominant role in the adsorption process. A wide range of materials can be used to remove nickel from solutions such as polyacrylonitrile composite nanofiber [12], maghemite nanoparticle (γ-Fe_3O_4) [13], dowex-50 ion-exchanger [14], *Litchi chinensis* seeds [15], chitosan beads [9], and wool chelating fibers [16].

Gel-type weak acid resin (110-H) is a polymeric material which contains the functional group (−COOH). This group has a proton that can be exchanged with many cations [17], and its oxygen atoms can be chelated with nickel ions. Its principal characteristics are great chemical and physical stabilities, high exchange capacity, good ability for regeneration, effective cheap, and easy to use. Therefore, it is a promising candidate to remove heavy metals from industrial wastewater. The adsorption process involves the variation of physicochemical parameters such as pH, temperature, and initial metal concentration. However, few studies have applied systematically statistical methods to investigate the combination of parameters that provides optimum adsorption conditions. RSM is proved to be an effective tool for the above-mentioned purpose. It is a collection of statistical and mathematical technique for developing, improving, and optimizing process conditions. Therefore, it is less time-consuming and more effective than any other conventional methods [18].

In this work, series of batch experiments were carried out to study the adsorption behavior. RSM was used to determine the optimization of adsorption conditions of Ni(II) on 110-H resin. The resins were characterized by Fourier transform infrared (FT-IR) and SEM analysis. FT-IR analyses is an important analytical technique for determination of adsorption mechanism. SEM images show the morphology and surface composition of 110-H resin and 110-H-Ni resin, after eluting 110-H-Ni resin. In addition, the equilibrium adsorption isotherm and thermodynamic parameters were also investigated. The experimental results may provide important information for the separation or removal of Ni(II) ion from aqueous solutions in the environment protection and wastewater treatment.

2. Materials and methods

2.1. Materials

110-H resin was provided by Nankai University, China. And the properties are shown in Table 1. The standard stock solutions were prepared by dissolving an appropriate amount of $NiCl_2{\cdot}6H_2O$ in deionizer water. HAc-NaAc buffer solutions with pH value of 3.00–7.00 were prepared from appropriate dilution of 0.4 mol/L HAc and 0.4 mol/L NaAc. $C_6H_{12}N_4$–HCl buffer solutions with pH 5.40 were prepared from appropriate dilution of 2.86 mol/L $C_6H_{12}N_4$ and concentrated HCl solutions. Natural water samples were collected from Hangzhou Coral sand reservoir and Erlongshan Reservoir. The chromophoric reagent of 0.1% xylenol orange solution was obtained by dissolving 0.1000 g xylenol orange powder into 100 mL deionized water. All other chemicals were the analytic-grade reagents.

2.2. Apparatus

The Ni(II) concentration was determined with Shimadzu UV-2550 ultraviolet–visible spectrophotometer.

Table 1
General description and properties of 110-H resin

Item	Property
Resin	Gel-type weak acid resin
Functional group	−COOH
Bead size (mm)	0.315–1.25
Total exchange capacity (mmol/mL)	≥4
Moisture content (%)	52–62
pH range	5–14

The 110-H resin was measured by BS 224S electronic balance (Sartorius Group, Germany). Mettler Toledo delta 320 pH meter was used for measuring pH of solutions. The samples were shaken in the DSHZ-300A and THZ-C-1 temperature-constant shaking machine. The water used in the present work was purified using a Mol research analysis type ultrapure water machine. IR spectra and scanning electron micrographs for the samples were obtained from a Nicolet 380 FT-IR spectrometer and a Phenom Pure SEM, respectively. Water samples were filtered through a 0.2-μm polyethersulfone (PES) vacuum filtration unit (Vivascience AG, Germany).

2.3. Resin adsorption and desorption experiments

Batch adsorption experiments were performed in the conical flasks containing 30 mL of adsorption solution and 15.0 mg of dried 110-H resin. Adsorption of Ni(II) from aqueous solution to the adsorbents was studied at various pH values in the HAc-NaAc buffer system. Adsorption experiments were conducted in a shaker of 100 rpm at different temperatures (ranging from 15 to 35˚C) for 24 h. The upper layer of clear solution was taken for analysis until reaching adsorption equilibrium.

Desorption experiments were performed immediately after the completion of the adsorption experiments. At the end of the adsorption experiments, the resins were separated from the aqueous solution by filtration, washed by deionized water, and agitated with different eluent solutions of various concentrations, at 100 rpm for 24 h at 298 K. The final metal ion concentration in the aqueous phase was similarly analyzed as described above.

Continuous packed bed studies were performed in a fixed-bed mini glass column (3 mm × 30 cm long) with 100.0 mg of resin. The 110-H resin in the column was presoaked for 24 h before the experiment. The Ni (II) solution with a known concentration and flow rate was passed continuously through the stationary bed of absorbent in down-flow mode. The experiment continued until a constant Ni(II) ion concentration was obtained. The column studies were performed at the optimum pH value determined from batch studies and at a constant temperature of 35˚C.

2.4. Characterization

IR spectra for the samples were obtained from a Nicolet 380 FT-IR spectrometer. Samples were dried before characterization using an infrared lamp to remove the adsorbed water. Scanning electron micrographs for the samples were obtained using a Phenom Pure SEM. The samples were dried to constant weight in a 100˚C oven.

2.5. Experimental design for RSM study

RSM was used to optimize the adsorption conditions of 110-H resin for Ni(II) from aqueous solutions. Factor combinations were obtained by the application of a Box–Behnken design using software Design-Expert. In this study, the variables such as temperature, pH, and initial Ni(II) concentration are selected as process parameters on the adsorption capacity of Ni(II) on 110-H resin. The levels and independent variables are shown in Table 2.

2.6. Analytical method

A solution containing a required amount of Ni(II) was added into a 25-mL colorimetric tube, and then, 2 mL of 0.1% xylenol orange solution and 10 mL $C_6H_{12}N_4$—HCl buffer solution (pH = 5.40) were added [19]. After the addition of purified water to the mark of the colorimetric tube, the absorbency was determined in a 1-cm colorimetric vessel on a Shimadzu UV-2550 UV–visible spectrophotometer at the wavelength of 578 nm and compared with the blank test. The adsorption capacity (Q, mg/g), distribution coefficient (D, mL/g), and desorption ratio (E, %) [20] were calculated with the following formulas:

$$Q = \frac{(C_0 - C_e)V}{m} \quad (1)$$

$$D = \frac{C_0 - C_e}{W \times C_e} V \quad (2)$$

$$E = \frac{C_d V_d}{(C_0 - C_e)} \times 100\% \quad (3)$$

Table 2
Experimental design of the adsorption of 110-H resin for Ni(II)

Symbols	Factors	Coded levels		
		−1	0	+1
A	Temperature (℃)	15	25	35
B	Initial pH	5	6	7
C	Initial Ni(II) concentration (mg/mL)	0.20	0.30	0.40

where C_0 and C_e are the initial and equilibrium concentrations of metal ion in solution (mg/mL); C_d is the concentration of metal ion in desorption solution; V and V_d are the total volume of solution and desorption solution (mL); and W is resin dry weight (g).

3. Results and discussion

3.1. Regression model equation and analysis of variance

The main objective of RSM was to determine regression model of adsorption process, and the quadratic model was used to find out the relationship between the response and variables in this article. According to experiment data, the final empirical model of Ni(II) adsorption on 110-H resin was described using Eq. (4):

$$\begin{aligned}\text{Adsorption Capacity} = {} & 163.39 + 39.20A + 29.40B \\ & + 8.41C + 1.37AB + 0.04AC \\ & - 3.64BC - 19.65A^2 - 26.16B^2 \\ & - 12.53C^2\end{aligned} \quad (4)$$

In order to ensure the adequacy of the employed model, an adequate fit of the model should be given to avoid poor or ambiguous results. The significance of quadratic regression model was tested by the values of F, P, and correlation coefficient, and the corresponding results of analysis of variance ANOVA are summarized in Table 3. The model F-value (61.88) and a very low p-value (<0.0001) implied that the model was highly significant for Ni(II) adsorption on 110-H resin. "Adequate Precision" measured the signal-to-noise ratio, which is desirable if greater than 4.0 is desirable [21]. "Adequate Precision" measured the signal-to-noise ratio, which is desirable if greater than 4.0. It is evident that the lack-of-fit value is insignificant, which demonstrates that the quadratic model for Ni(II) adsorption over 110-H resin is very valid. The value of determination coefficient ($R^2 = 0.9876$) of Eq. (4) indicates that the regression model is best suited for predicting the performance of Ni(II) adsorption with 110-H resin. As can be seen from Table 3, all the p-values of A, B, A^2, B^2, and C^2 are less than 0.05, indicating that these variables are significant and have great influence on Ni(II) adsorption capacity.

3.2. The optimization of adsorption conditions

The results of the adsorption capacity affected by temperature, pH, and initial Ni(II) concentration are shown in panels a, b, and c, respectively, of Fig. 1. Fig. 1 illustrates the mutual interactive effects of the combination of independent variables on Ni(II) adsorption capacity in the manner of 3D surface plots, which were represented as a function of two factors by holding the other factor at level zero. From the 3D surface plots, the optimal values of the parameters could be observed.

Fig. 1(a) indicated that adsorption capacity increased within the temperature range of 15–35℃, indicating that the adsorption process is an endothermic process. The results show that adsorption capacity for Ni(II) increases rapidly with the increase in initial pH from 5.0 to 6.5 in the HAc-NaAc buffer solutions, and then decreased from 6.5 to 7.0 under the experimental conditions. As seen from Fig. 1(b), within the range of experimental variables, it appears that higher temperature and initial Ni(II) concentration are beneficial for the adsorption capacity during the adsorption process, which is a significant effect on the adsorption capacity of Ni(II) on 110-H resin. Fig. 1(c) suggests that increasing the concentration of Ni(II) within the tested range encourages the adsorption capacity for Ni(II) under the experimental conditions. In addition, increasing initial Ni(II) concentration enlarges the number of collisions between Ni(II) ions and sorbent, thus enhancing the adsorption process.

The RSM-guided optimization demonstrated that the optimal adsorption conditions for Ni(II) on 110-H resin from aqueous solutions are temperature of 35℃, pH of 6.57, and initial Ni(II) concentration of 0.33 mg/mL, and the predicted adsorption capacity reached 192.88 mg/g. Three batch experiments of the

Table 3
ANOVA results of response surface quadratic model according to adsorption capacity of 110-H resin for Ni(II)

Source	Sum of squares	Degree of freedom	Mean square	*F*-value	Prob > *F*
Model	25553.16	9	2839.24	61.88	<0.0001
A	12293.90	1	12293.90	267.94	<0.0001
B	6915.47	1	6915.47	150.72	<0.0001
C	565.49	1	565.49	12.32	0.0099
AB	7.48	1	7.48	0.16	0.6984
AC	0.62	1	0.62	0.014	0.9104
BC	53.00	1	53.00	1.16	0.3181
A^2	1625.16	1	1625.16	35.42	0.0006
B^2	2881.73	1	2881.73	62.81	<0.0001
C^2	666.74	1	666.74	14.53	0.0066
Residual	321.18	7	45.88		
Lack-of-fit	321.18	3	107.06		
Pure error	0.000	4	0.000		

Notes: $R^2 = 0.9876$; $R^2_{adj} = 0.9716$; adequate precision = 26.41.

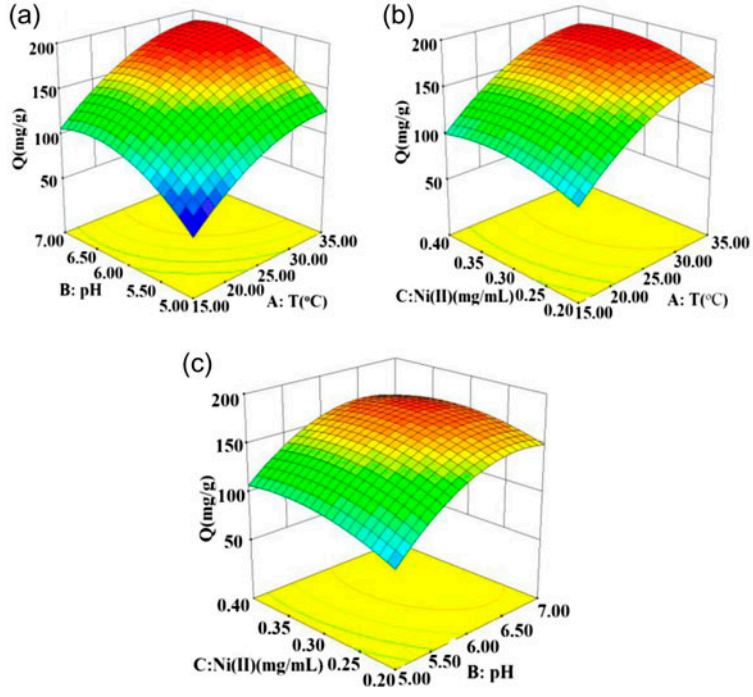

Fig. 1. Three-dimensional plots showing effects of (a) pH and temperature, (b) temperature and initial Ni(II) concentration, and (c) pH with initial Ni(II) concentration interactions on adsorption capacity of 110-H resin for Ni(II).

adsorption of 110-H resin for Ni(II) were implemented using the predicted optimum condition in order to validate the developed mathematical models. The mean value of adsorption capacity was 188.5 mg/g, in close agreement with the predicted value (192.88 mg/g), indicating that the developed model was adequate for predicting the adsorption conditions of 110-H resin for Ni(II) from aqueous solutions.

3.3. Adsorption kinetics

In order to find out the equilibrium time for the maximum adsorption and to determine the rate-limiting step of the adsorption process, the change in the adsorption capacity of Ni(II) on 110-H resin at different times was recorded. The results are shown in Fig. 2. It can be seen in Fig. 2 that the equilibrium state was not reached for 26 h. As the temperature

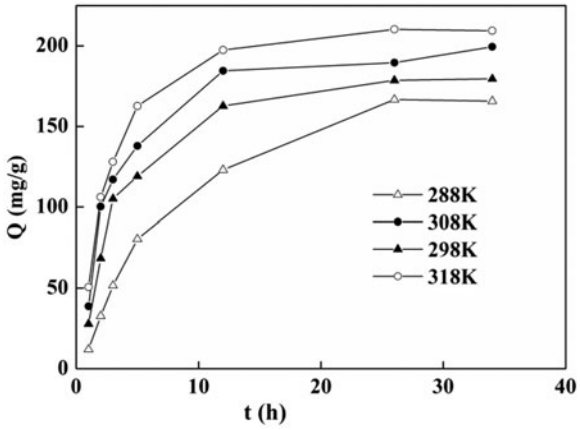

Fig. 2. Adsorption amount of different temperatures (resin 15.0 mg, C_0 = 0.33 mg/mL, pH = 6.57).

increased from 288 to 318 K, the equilibrium adsorption capacity exhibited the same trend. A higher adsorption capacity at higher temperature suggests that the Ni(II) adsorption onto the 110-H resin is a temperature-dependent process [22].

To further investigate the rate-controlling step of the Ni(II) adsorption process, the kinetic sorption data were treated with two simplified kinetic models including Lagergren-first-order kinetics model and pseudo-second-order kinetics model. The Lagergren first-order kinetics model [23] is expressed as follows:

$$\lg (Q_e - Q_t) = \lg Q_1 - \frac{k_1 t}{2.303} \quad (5)$$

The pseudo-second-order model [24] is expressed as follows:

$$\frac{t}{Q_t} = \frac{1}{k_2 Q_2^2} + \frac{t}{Q_2} \quad (6)$$

where k_1 (min^{-1}) and k_2 (g/mg min) are the rate constants of the first-order kinetics and the second-order kinetics, respectively, and Q_e (mg/g) and Q_t (mg/g) are the amounts of metal ion adsorbed at equilibrium and time t (min), respectively. Q_1 and Q_2 are the calculated adsorption capacities of the Lagergren first-order model and the pseudo-second-order model (mg/g), respectively.

The kinetic parameters are represented in Table 4, the experimental data for adsorption of Ni(II) on 110-H showed that the correlation coefficient (R_2^2) for the pseudo-second-order model is better than the correlation coefficient (R_1^2) for the Lagergren first-order model [22]. Moreover, the experimentally calculated capacity of the pseudo-second-order model generates good fittings which indicated that the interactions would follow the pseudo-second-order kinetics. In other words, the pseudo-second-order model can describe the Ni(II)/110-H adsorption system studied in our work, and the rate-controlling step of the adsorption process is governed by chemisorption [25].

According to the Brykina method [26], the adsorption rate constant k can be calculated from the following formula:

$$-\ln (1 - F) = kt \quad (7)$$

$$F = \frac{Q_t}{Q_e} \quad (8)$$

where F is the fractional attainment of equilibrium and Q_t (mg/g) and Q_e (mg/g) are the adsorption amounts at certain time and at equilibrium time, respectively. The experimental results were in accord with the equation, and a straight line is obtained by plotting −ln (1–F) vs. t. Therefore, the adsorption rate constant could be found from the slope of the straight line, which was $k_{298\,K} = 4.041 \times 10^{-5}\ s^{-1}$. The correlation coefficient (R^2 = 0.961) was obtained via linear fitting. The other results are listed in Table 5. The apparent rate constant clearly increases with an increasing temperature. According to the Boyd equation, it could be deduced from the linear relationship of −ln (1–F) vs. t that the liquid film spreading was

Table 4
The first-order and second-order kinetics constants for adsorption of Ni(II) on 110-H resin

		Lagergren first-order model			Pseudo-second-order model		
T (K)	Q_e (mg/g)	k_1 (min^{-1})	Q_1 (mg/g)	R_1^2	k_2 (g/mg min)	Q_2 (mg/g)	R_2^2
288	165.7	0.0019	199.5	0.9776	0.0044	227.3	0.9805
298	179.6	0.0016	144.5	0.9230	0.0047	212.8	0.9830
308	199.4	0.0018	154.9	0.9624	0.0044	227.3	0.9924
318	209.3	0.0019	147.9	0.9009	0.0043	232.6	0.9967

Table 5
Adsorption rate constants of 110-H resin for Ni(II) under various temperatures

T (K)	Linearity relation of $-\ln(1-F)$ and t	K	R^2
288	$y = 0.1070x + 0.0260$	$K = 2.972 \times 10^{-5}\ s^{-1}$	$R^2 = 0.974$
298	$y = 0.1485x + 0.1741$	$K = 4.041 \times 10^{-5}\ s^{-1}$	$R^2 = 0.961$
308	$y = 0.1585x + 0.2363$	$K = 4.402 \times 10^{-5}\ s^{-1}$	$R^2 = 0.971$
318	$y = 0.1685x + 0.2919$	$K = 4.680 \times 10^{-5}\ s^{-1}$	$R^2 = 0.960$

the predominating step of the adsorption process. According to the Arrhenius equation [27],

$$\lg k = -\frac{E_a}{2.303RT} + \lg A \tag{9}$$

where E_a is the Arrhenius activation energy for the adsorption process, indicating the minimum energy, A is the Arrhenius factor, R is the gas constant (8.314 J/(mol K)), k is the adsorption rate constant, and T is the solution temperature. As could be observed in Fig. 3, E_a and A values can be estimated from slope and intercept values of this plot lg k vs. T^{-1}, respectively. The slope of the straight line was $K_{slope} = -0.5125$. The correlation coefficient of the straight line $R^2 = 0.990$ was achieved. The apparent activation energy E_a was 9.81 kJ/mol, which could be considered as a low energy barrier in this study [28]. There are two main types of adsorption: physical and chemical. Usually, the activation energy for physical adsorption is not more than 4.2 kJ/mol, since the forces involved in this process are weak. Chemical adsorption is specific and involves forces much stronger than those in physical adsorption. With chemical adsorption, the rate varies with temperature according to a finite activation energy (8.4–83.7 kJ/mol) in the Arrhenius equation [29]. The apparent activation energy of 9.81 kJ/mol for Ni(II) removal is within the finite activation energy range of chemical adsorption. Therefore, this result confirms that the rate-determining step for Ni(II) removal from aqueous solution was chemical adsorption.

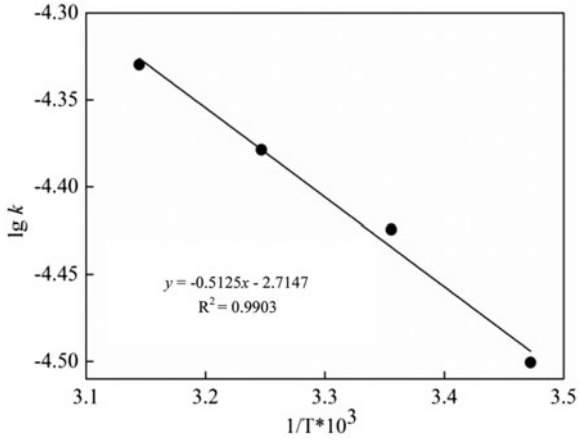

Fig. 3. Relationship between l g k and $1/T$ (resin = 30.0 mg, C_0 = 0.33 mg/mL).

3.4. Adsorption isotherm

To further explore the adsorption mechanism, we used Langmuir [30] and Freundlich [31] isotherm models to analyze the equilibrium data for the experiments carried out at different temperatures under pH 6.57. The Langmuir isotherm is based upon an assumption of monolayer adsorption onto a surface, which contains a finite number of adsorption sites with uniform energies of adsorption and no transmigration of adsorbate in the plane of the surface. The Freundlich isotherm model assumes heterogeneous surface energies in which energy term in Langmuir equation varies as a function of surface coverage [32]. In this paper, both models are used to describe the relationship between the amount of Ni(II) adsorbed on 110-H resin and its equilibrium concentration in solution at three different temperatures (288, 298, and 308 K). The Langmuir and Freundlich can be expressed as follows.

Langmuir isotherm:

$$\frac{C_e}{Q_e} = \frac{C_e}{Q_0} + \frac{1}{Q_0 K_L} \tag{10}$$

Freundlich isotherm:

$$\lg Q_e = \left(\frac{1}{n}\right) \times \lg C_e + \lg K_f \tag{11}$$

where Q_e is the equilibrium sorption amount, C_e is the equilibrium concentration, Q_0 is the maximum

adsorption capacity of Langmuir, K_L is Langmuir constants, n is a constant indicating the Freundlich isotherm curvature, and K_f is the Freundlich sorption coefficients.

K_L (mL/mg) is Langmuir constant related to the energy of adsorption and increases with increasing strength of the adsorption bond, which is used to evaluate the dimensionless parameter known as separation factor (R_L) using the following equation [33]:

$$R_L = \frac{1}{1 + K_L C_0} \tag{12}$$

where C_0 is the initial concentration of Ni(II) and R_L depicts whether the monolayer adsorption predicted by the Langmuir model is irreversible ($R_L = 0$), favorable ($0 < R_L < 1$), linear ($R_L = 1$), or unfavorable ($R_L > 1$) [34].

The Langmuir and Freundlich isotherm constants are calculated and listed in Table 6. Obviously, with a higher R^2 value, the Langmuir model was found to be a better fit for the experimental data than the Freundlich model. The adsorption constants evaluated from the isotherms and their correlation coefficients are shown in Table 6. This suggested that the adsorption of Ni(II) by 110-H resin was monolayer type and agreed with the observation that the metal ion adsorption from an aqueous solution usually forms a layer on the adsorbent surface [17]. The increase of the Q_m value with the temperature rise indicates that the process needs thermal energy (endothermic) and there is a chemical interaction between adsorbent and adsorbate [22]. The calculated values of R_L were between 0 and 1 (Table 6), indicating that the adsorption of Ni (II) on 110-H resin is favorable.

3.5. Thermodynamic parameters

In any adsorption procedure, both energy and entropy considerations should be taken into account to determine which process will take place spontaneously. The amounts of Ni(II) ions adsorbed at equilibrium at different temperatures, which were 288, 298, and 308 K, have been examined to obtain thermodynamic parameters for the adsorption system. Thermodynamic parameters such as the Gibb's free energy (ΔG), enthalpy (ΔH), and entropy (ΔS) for the adsorption process can be determined by the following equations [35], which can be used to calculate the enthalpy changes associated with the adsorption process of the metal ions.

$$\lg D = -\frac{\Delta H}{2.303\ \mathrm{RT}} + \frac{\Delta S}{2.303\ R} \tag{13}$$

where R is the universal gas constant, D is the distribution coefficient, and T (K) is the absolute temperature. The plot of lg D vs. $1/T$ gives a straight line, from which ΔH (the enthalpy variation) and ΔS (the entropy variation) are deduced from the slope and intercept of the line, respectively. The free energy variation ΔG is calculated from the following equation:

$$\Delta G = \Delta H - T\Delta S \tag{14}$$

The negative value of ΔG (kJ/mol) (288 K, −16.56; 298 K, −17.67; 308 K, −18.79) indicates that the Ni(II) adsorption on the 110-H resin is feasible and thermodynamically spontaneous. The decrease in magnitude of ΔG as the temperature rises from 288 to 318 K confirms that the adsorption is favorable at higher temperatures, due to the greater swelling of the resin and increased diffusion of metal ions into the resin [36]. The positive value of $\Delta H = 15.47$ kJ/mol suggests that the Ni(II) adsorption is an endothermic process. In addition, the values of $\Delta S = 111.21$ J/(K mol) are found to be positive due to the exchange of the metal ions with more mobile ions present on the exchanger, which would cause increase in the entropy, during the adsorption process [37] (see Table 7).

3.6. Elution

Whether an adsorbent is economically attractive in removal of metal ions from aqueous solution depends not only on the adsorptive capacity, but also on how

Table 6
Isotherm constants for the adsorption of Ni(II) on 110-H resin at various temperatures

	Langmuir isotherm				Freundlich isotherm	
T (K)	Q_m (mg/g)	R^2	K_L	R_L	n	R^2
288	176.4	0.9945	13.25	0.0364–0.0537	11.38	0.9167
298	182.4	0.9961	25.00	0.0196–0.0292	3.34	0.9949
308	188.5	0.9904	23.50	0.0208–0.0317	2.11	0.9510

Table 7
Thermodynamic data calculated for adsorption of Ni(II) on 110-H resin

		ΔG (kJ/mol)		
ΔH (kJ/mol)	ΔS (J/Kmol)	T = 288 K	T = 298 K	T = 308 K
15.47	111.21	−16.56	−17.67	−18.79

well the adsorbent can be easily desorbed. In this work, different concentrations of HCl were employed in range from 0.5 to 3.0 mol/L and the results were obtained. The percentages of elution are 90.76, 92.26, 96.34, 98.63, 100, and 87.51 for 0.5, 1.0, 1.5 1.8, 2.0, and 3.0 mol/L HCl concentration, respectively. It was evident from data that the maximum percentage of elution for Ni(II) was obtained using 2.0 mol/L HCl solution as an eluant.

3.7. Dynamic adsorption and desorption curve

Batch experimental data are often difficult to apply directly to fixed-bed adsorption because isotherms are unable to give accurate data for a dynamically operated column. The fixed-bed column operation allows more efficient utilization of the adsorptive capacity than the batch process.

The performance of packed beds is described through the concept of the breakthrough curve. It shows the loading behavior of Ni(II) to be removed from solution in a fixed bed. Furthermore, it is usually expressed in terms of adsorbed Ni(II) concentration (C_{ad} = inlet Ni(II) concentration (C_0) outlet Ni(II) concentration (C_e)) or normalized concentration defined as the ratio of effluent Ni(II) concentration to inlet Ni (II) concentration (C_e/C_0) as a function of time or volume of effluent for a given bed height. Successful design of a column adsorption process requires prediction of the concentration vs. time profile or breakthrough curve for the effluent.

The dynamic adsorption test was conducted using a glass column packed with 300 mg newly prepared 110-H resin at room temperature. After the column was conditioned, a solution containing 0.33 mg/mL Ni(II) was continuously fed into the column at a constant flow rate of 0.417 mL/min. The effluents from the column were analyzed quantitatively using the above-mentioned method. Breakthrough data were acquired by plotting the volume of solution passing through the column versus the concentration of Ni(II) in the effluent. Until the concentration of metal ions in the effluent $C_e = C_0$, a plot of C_e/C_0 versus the volume of effluent gave a typical breakthrough curve. As shown in Fig. 4, the breakthrough point of adsorption at 175 mL, when $V < 175$ mL, the metal ions were almost completely adsorbed, V = 850 mL, Ni(II) was almost completely outflow. This suggested that the dynamic adsorption has reached saturation.

Efficient elution of adsorbed solute from 110-H resin in column was essential to ensure the reuse of 110-H resin for repeated adsorption/desorption cycles. With respect to the stripping of Ni(II) from 110-H resin, 2.0 mol/L HCl eluant was employed. Desorption curve was plotted using the effluent concentration (C_e) vs. elution volume from the column at a certain flow rate. It could be seen from Fig. 5 that the desorption flow rate was less, so the volume of elution was less. This contributes easy handling and high concentration for economic recovery of Ni(II).

It was observed that the total volume of eluant was 40 mL, after which further desorption was negligible. Therefore, the 2.0 mol/L HCl eluant could result to easy handling and removal of Ni(II).

Data on the adsorption capacity and desorption ratio of Ni(II) by the recent reported adsorbents [12–15,9,23,38–40,16] are listed in Table 8. 110-H resin exhibits a higher adsorption capacity of Ni(II) than other materials and a 100% desorption ratio.

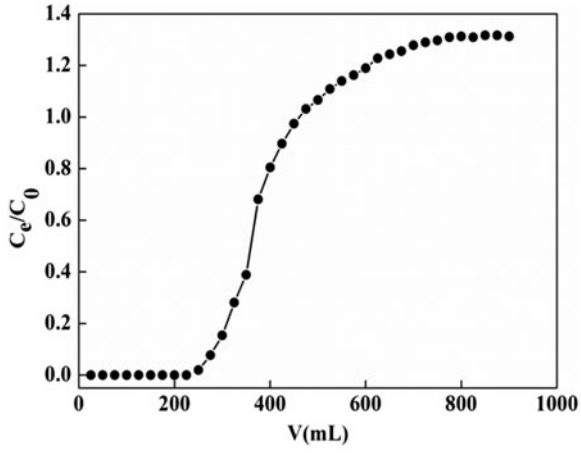

Fig. 4. Dynamic adsorption curve (resin = 300 mg, C_0 = 0.33 mg/mL, flow rate = 0.417 mL/min).

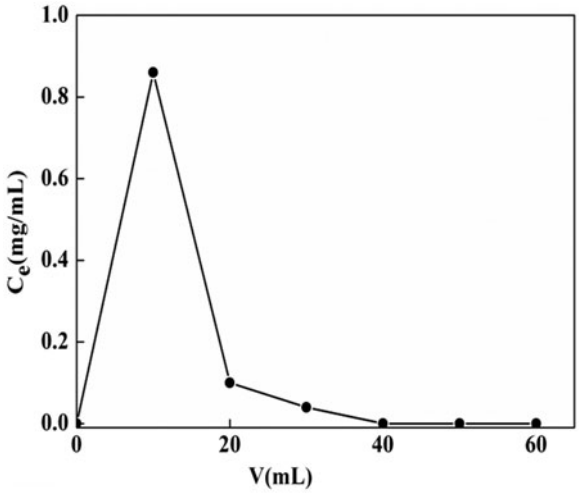

Fig. 5. Dynamic desorption curve (resin = 300 mg, C_{HCl} = 2.0 mol/L, flow rate = 0.400 mL/min).

3.8. Application to samples of natural waters

At optimum adsorption conditions (initial Ni(II) concentration of 0.33 mg/mL, 35℃), adsorption experiments for the removal of Ni(II) from Hangzhou Coral sand and Erlongshan Reservoir water samples had been carried out using 110-H resin. Adsorption experiments were performed in the conical flasks containing 30 mL adsorption solutions (water samples and 5 mL nickel solutions (2.0 mg/mL)) and 15.0 mg of dried 110-H resin. Adsorption experiments were conducted in a shaker of 100 rpm at 35℃ for 24 h. The adsorption capacity of Ni(II) was 151.6 and 165.8 mg/g for Hangzhou Coral sand and Erlongshan Reservoir water samples, respectively. Therefore, the 110-H resin has been successfully applied in the removal of Ni(II) in natural water samples.

3.9. Infrared spectra analysis

IR analysis is an important analytical technique for determination of adsorption mechanism. It was deduced that the adsorption of Ni(II) by 110-H ($\Delta H > 0$) resin was a chemical process. Therefore, the functional groups of 110-H, C=O, C–OH, and Ni(II) are supposed to form chemical bonds. To identify the possibility of Ni(II) bonding to resin, IR spectra were obtained for 110-H resin before and after Ni(II) adsorption, after elution, as shown in Fig. 6. It should be noticed that the bands at 1,734 and 1,591 cm^{-1} are indications of C=O. It was found that the characteristic absorption peak of the bond C=O (1,734 cm^{-1}) weakened after Ni(II) adsorption, and the new peak formed at 1,591 cm^{-1}. The characteristic peak of the bond C–OH shifts from 1,394 to 1,406 cm^{-1}. These results showed that there were coordination bonds between

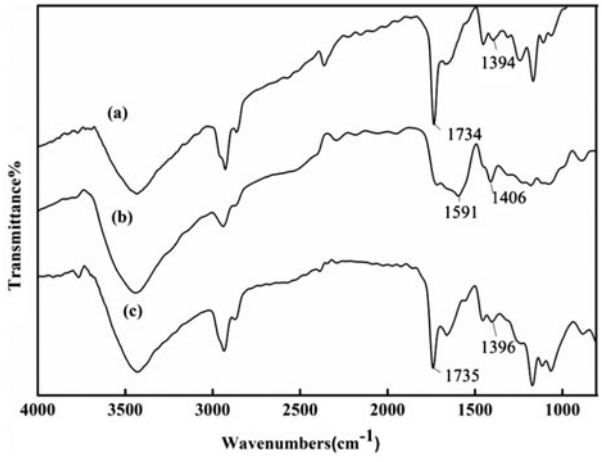

Fig. 6. IR spectra of 110-H resin: (a) before adsorption, (b) after adsorption, and (c) after elution.

Table 8
Comparison of Ni(II) adsorption on 110-H resin and other sorbents

Adsorbents	Adsorption capacities (mg/g)	Desorption ratio	References
PAN/SiO_2/APTES	138.7	–	[12]
Maghemite nanoparticle	114.9	–	[13]
Dowex-50 ion-exchanger	83.33	93	[14]
Litchi chinensis seeds	66.62	–	[15]
Chitosan beads	55.6	66.49	[9]
SPCTO	51.814	95	[23]
Montmorillonite nanocomposites	46.94	98	[38]
Graphene nanosheet/δ-MnO_2	46.6	97.6	[39]
Ni-doped Fe_2O_3	42	–	[40]
Wool chelating fibers	15.3	91.7	[16]
110-H resin	188.5	100	This work

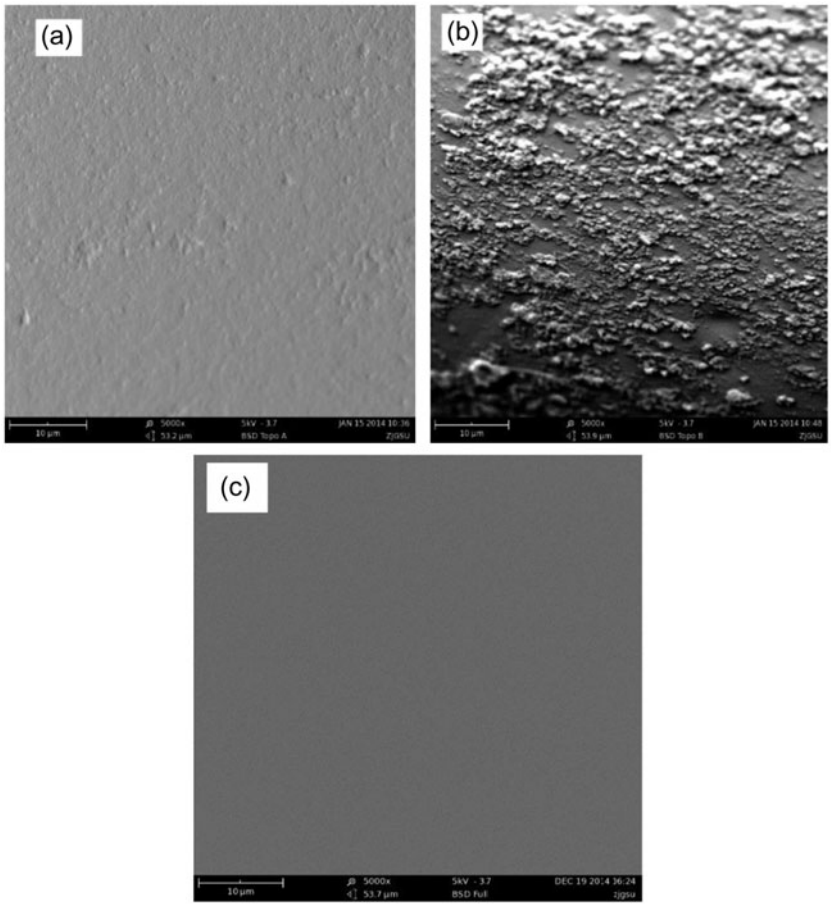

Fig. 7. SEM images of (a) 110-H resin and (b) after Ni(II) adsorption, and (c) after Ni(II) elution.

oxygen atoms and Ni(II) and that H of C–OH had been exchanged with the formation of a complex compound [32]. These results revealed that the C=O groups participated in the adsorption process. By comparing with the curve of 110-H resin and after Ni(II) elution, the characteristic absorption peak of the bond C=O (1,734 cm^{-1}) and C–OH (1,394 cm^{-1}) was found to slightly weaken after Ni(II) elution. Therefore, 110-H resins have good ability for regeneration and efficient reusable ability toward Ni(II).

3.10. SEM analysis

After adsorption of as-prepared resin with Ni(II) solution, their color changed a little and the resin was studied by microscopic techniques (Fig. 7). The studies performed by means of optical microscope also confirmed that the 110-H resin has no pores in-house in the dry condition. The SEM micrographs are widely used to observe the morphological features and surface characteristics of the adsorbent materials. Comparing the surface of 110-H resin with Ni(II)-loaded resin, the surface of the 110-H resins turned thicker and granular. The results showed that Ni(II) ions were adsorbed by 110-H resin. Comparing the surface of 110-H resin with Ni(II)-eluted resin, it is found that Ni(II) ions had been completely eluted. Therefore, 110-H resin have good ability for regeneration and efficient reusable ability toward Ni(II).

4. Conclusions

In this study, batch adsorption experiments for the removal of Ni(II) from aqueous solutions had been carried out using 110-H resin. The RSM analysis demonstrates that optimum adsorption conditions were 35℃, pH 6.57, and initial Ni(II) concentration of 0.33 mg/mL. At optimum adsorption conditions, the adsorption capacity of Ni(II) reached 188.5 mg/g, close to the value predicted by the model (192.88 mg/g). Isothermal studies showed that the adsorption process of 110-H resin for Ni(II) obeys the

Langmuir model. Ni(II) adsorbed on 110-H resin can be eluted by 2.0 mol/L HCl solution, and the 110-H resin can be regenerated and reused. The SEM and IR spectra analyses were examined to determine the adsorption mechanism of 110-H resin. In conclusion, the results of this investigation supports that the 110-H resin is an effective adsorbent to remove and recover Ni(II) from aqueous solutions in the environmental protection and wastewater treatments.

Acknowledgment

This study was supported by PhD Programs Foundation of Ministry of Education of China (No.: 20133326110006), the Special Major Science and Technology Project of Zhejiang Province, China, (No.: 2012C03002-2), and Key Laboratory of Advanced Textile Materials and Manufacturing Technology (Zhejiang Sci-Tech University), Ministry of Education (No.: 2013006).

References

[1] D.W. O'Connell, C. Birkinshaw, T.F. O'Dwyer, Heavy metal adsorbents prepared from the modification of cellulose: A review, Bioresour. Technol. 99 (2008) 6709–6724.
[2] S. Malamis, E. Katsou, A review on zinc and nickel adsorption on natural and modified zeolite, bentonite and vermiculite: Examination of process parameters, kinetics and isotherms, J. Hazard. Mater. 252–253 (2013) 428–461.
[3] M.A. Khan, M. Ngabura, T.S. Choong, H. Masoos, L.A. Chuah, Biosorption and desorption of Nickel on oil cake: Batch and column studies, Bioresour. Technol. 103 (2012) 35–42.
[4] N.R. Axtell, S.P. Sternberg, K. Claussen, Lead and nickel removal using Microspora and *Lemna minor*, Bioresour. Technol. 89 (2003) 41–48.
[5] N. Akhtar, J. Iqbal, M. Iqbal, Removal and recovery of nickel(II) from aqueous solution by loofa sponge-immobilized biomass of *Chlorella sorokiniana*: characterization studies, J. Hazard. Mater. 108 (2004) 85–94.
[6] V.N. Tirtom, A. Dinçer, S. Becerik, T. Aydemir, A. Çelik, Comparative adsorption of Ni(II) and Cd(II) ions on epichlorohydrin crosslinked chitosan-clay composite beads in aqueous solution, Chem. Eng. J. 197 (2012) 379–386.
[7] H. Hyung, J.-H. Kim, A mechanistic study on boron rejection by sea water reverse osmosis membranes, J. Membr. Sci. 286 (2006) 269–278.
[8] B.R. Reddy, D.N. Priya, Chloride leaching and solvent extraction of cadmium, cobalt and nickel from spent nickel-cadmium, batteries using Cyanex 923 and 272, J. Power Sources 161 (2006) 1428–1434.
[9] A. Eser, V. Nüket Tirtom, T. Aydemir, S. Becerik, A. Dinçer, Removal of nickel(II) ions by histidine modified chitosan beads, Chem. Eng. J. 210 (2012) 590–596.
[10] E. Pehlivan, T. Altun, Ion-exchange of Pb^{2+}, Cu^{2+}, Zn^{2+}, $Cd^{2+}$and Ni^{2+} ions from aqueous solution by Lewatit CNP 80, J. Hazard. Mater. 140 (2007) 299–307.
[11] A.A. Hekmatzadeh, A. Karimi-Jashani, N. Talebbeydokhti, B. Kløve, Modeling of nitrate removal for ion exchange resin in batch and fixed bed experiments, Desalination 284 (2012) 22–31.
[12] A. Dastbaza, A.R. Keshtkar, Adsorption of Th^{4+}, U^{6+}, Cd^{2+}, and Ni^{2+}, from aqueous solution by a novel modified polyacrylonitrile composite nanofiber adsorbent prepared by electrospinning, Appl. Surf. Sci. 293 (2014) 336–344.
[13] P. Panneerselvam, N. Morad, Y.L. Lim, Separation of Ni(II) ions from aqueous solution onto maghemite nanoparticle (γ-Fe_3O_4) enriched with clay, Sep. Sci. Technol. 48 (2013) 2670–2680.
[14] R. Kumar, M. Kumar, R. Ahmad, M.A. Barakat, l-Methionine modified Dowex-50 ion-exchanger of reduced size for the separation and removal of Cu(II) and Ni(II) from aqueous solution, Chem. Eng. J. 218 (2013) 32–38.
[15] J.G. Flores-Garnica, L. Morales-Barrera, G. Pineda-Camacho, E. Cristiani-Urbina, Biosorption of Ni(II) from aqueous solutions by *Litchi chinensis* seeds, Bioresour. Technol. 136 (2013) 635–643.
[16] M. Monier, D.M. Ayad, A.A. Sarhan, Adsorption of Cu(II), Hg(II), and Ni(II) ions by modified natural wool chelating fibers, J. Hazard. Mater. 176 (2010) 348–355.
[17] C.H. Xiong, C.P. Yao, L. Wang, J.J. Ke, Adsorption behavior of Cd (II) from aqueous solutions onto gel-type weak acid resin, Hydrometallurgy 98 (2009) 318–324.
[18] M.M. Song, C. Branford-White, H.L. Nie, L.M. Zhu, Optimization of adsorption conditions of BSA on thermosensitive magnetic composite particles using response surface methodology, Colloids Surf. B 84 (2011) 477–483.
[19] C.H. Xiong, C.P. Yao, Ion exchange recovery of nickel (II) macroporous weak acid resin (D151 resin), Indian J. Chem. Technol. 18 (2011) 13–20.
[20] C.S. Yu, H.P. Liu, Y.Q. Li, Y.G. Zu, Preparation and characterization of degradable cellulose-based macroporous resin, Polym. Int. 61 (2012) 994–1001.
[21] J.H. Zhang, S.X. Chen, R. Yang, Y.Y. Yan, Biodiesel production from vegetable oil using heterogenous acid and alkali catalyst, Fuel 89 (2010) 2939–2944.
[22] C.H. Xiong, Q. Jia, X.Y. Chen, G.T. Wang, C.P. Yao, Optimization of polyacrylonitrile-2-aminothiazole resin synthesis, characterization, and its adsorption performance and mechanism for removal of Hg(II) from aqueous solutions, Ind. Eng. Chem. Res. 52 (2013) 4978–4986.
[23] W. Plazinsk, Applicability of the film-diffusion model for description of the adsorption kinetics at the solid/solution interfaces, Appl. Surf. Sci. 256 (2010) 5157–5163.
[24] A.E. Ofomaja, E.B. Naidoo, S.J. Modise, Dynamic studies and pseudo-second-order modeling of coper(II) biosorption onto pine cone powder, Desalination 251 (2010) 112–122.
[25] N. Dizge, B. Keskinler, H. Barlas, Sorption of Ni(II) ions from aqueous solution by Lewatit cation-exchange resin, J. Hazard. Mater. 167 (2009) 915–926.

[26] D. Zhang, M. Wang, G.J. Ren, E.J. Song, Preparation of biomorphic porous calcium titanate and its application for preconcentration of nickel in water and food samples, Mat. Sci. Eng. C-Mater. 33 (2013) 4677–4683.
[27] C.H. Xiong, Z.W. Zheng, Evaluation of D113 cation exchange resin for the removal of Eu(III) from aqueous solution, J. Rare Earths 28 (2010) 862–867.
[28] A. Demirbas, E. Pehlivan, F. Gode, T. Altun, G. Arslan, Adsorption of Cu(II), Zn(II), Ni(II), Pb(II), and Cd(II) from aqueous solution on Amberlite IR-120 synthetic resin, J. Colloid Interface Sci. 282 (2005) 20–25.
[29] M. Kragović, A. Daković, M. Marković, J. Krstić, G.D. Gatta, N. Rotiroti, Characterization of lead sorption by the natural and Fe(III)-modified zeolite, Appl. Surf. Sci. 283 (2013) 764–774.
[30] I. Langmuir, Adsorption of gases on plain surface of glass mica platinum, J. Am. Chem. Soc. 40 (1918) 1361–1403.
[31] H.Z. Freundlich, über die adsorption in lösungen (Uber die adsorption in losungen), Z. Phys. Chem. (J. Phys. Chem.) 57 (1906) 385–470.
[32] C.H. Xiong, R. Chen, Use of gel-type weak acid resin for the adsorption of La(III) from aqueous solution, Indian J. Chem. Technol. 19 (2012) 392–398.
[33] M. El Haddad, A. Regti, R. Slimani, S. Lazar, Assessment of the biosorption kinetic and thermodynamic for the removal of safranin dye from aqueous solutions using calcined mussel shells, J. Ind. Eng. Chem. 20 (2014) 717–724.
[34] O. Moradi, A. Fakhri, S. Adami, S. Adami, Isotherm, thermodynamic, kinetics, and adsorption mechanism studies of ethidium bromide by single-walled carbon nanotube and carboxylate group functionalized single-walled carbon nanotube, J. Colloid Interface Sci. 395 (2013) 224–229.
[35] N. Ünlü, M. Ersoz, Adsorption characteristics of heavy metal ions onto a low cost biopolymeric sorbent from aqueous solutions, J. Hazard. Mater. 136 (2006) 272–280.
[36] S.A. Ali, O.C. Al Hamouz, N.M. Hassan, Novel cross-linked polymers having pH-responsive amino acid residues for the removal of Cu^{2+} from aqueous solution at low concentrations, J. Hazard. Mater. 47 (2013) 248–249.
[37] M.R. Gandhi, N. Viswanathan, S. Meenakshi, Synthesis and characterization of a few amino-functionalized copolymeric resins and their environmental applications, Ind. Eng. Chem. Res. 51 (2012) 5677–5684.
[38] A. Barati, M. Asgari, T. Miri, Z. Eskandari, Removal and recovery of copper and nickel ions from aqueous solution by poly(methacrylamide-co-acrylic acid)/montmorillonite nanocomposites, Environ. Sci. Pollut. Res. Int. 20 (2013) 6242–6255.
[39] Y.M. Ren, N. Yan, Q. Wen, Z.J. Fan, T. Wei, M.L. Zhang, M. Jun, MaGraphene/δ-MnO_2 composite as adsorbent for the removal of nickel ions from wastewater, Chem. Eng. J. 175 (2013) 1–7.
[40] O.M. Lemine, I. Ghiloufi, M. Bououdina, L. Khezami, M.O. M'hamed, A.T. Hassan, Nanocrystalline Ni doped α-Fe_2O_3 for adsorption of metals from aqueous solution, J. Alloys Compd. 588 (2014) 592–595.